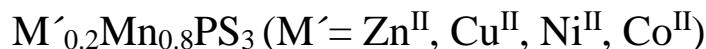


Magnetic Behavior of Bimetallic Layered Phases



P. Fuentealba^{1,2}, C. Cortes^{1,2}, J. Manzur^{2,3}, V. Paredes-García^{2,4}, D. Venegas-Yazigi^{2,5}, I. D. A. Silva⁶, R. C. de Santana^{7*}, C. J. Magon⁶, E. Spodine^{1,2*}.

¹Facultad de Ciencias Químicas y Farmacéuticas, Universidad de Chile, Santiago, Chile.

²CEDENNA, Santiago, Chile.

³Facultad de Ciencias Físicas y Matemáticas, Universidad de Chile, Santiago, Chile.

⁴ Departamento de Ciencias Químicas, Universidad Andrés Bello, Santiago, Chile.

⁵Facultad de Química y Biología, Universidad de Santiago de Chile, Santiago, Chile.

⁶Instituto de Física de São Carlos, Universidade de São Paulo, São Carlos, Brasil.

⁷Instituto de Física, Universidade Federal de Goiás, Goiânia, Brasil.

Fig. S1. Arrangement of Mn(II) ions and vacancies in the potassium precursor $K_{0.4}Mn_{0.8}PS_3 \cdot H_2O$, as determined by neutron diffraction (left) [^{1,2}]; and proposed arrangement for Mn(II) and secondary transition metal ions in the studied bimetallic phases (right)

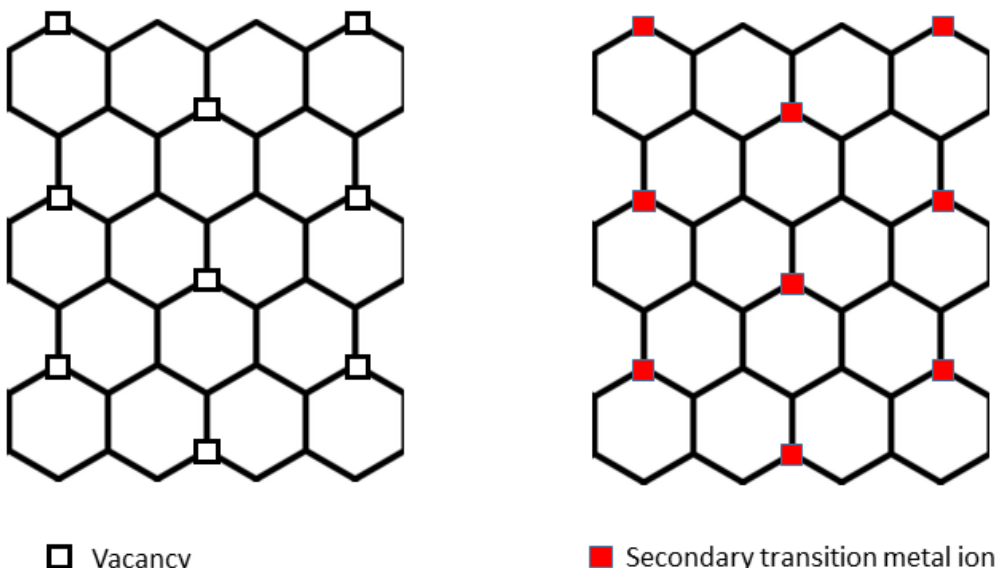


Fig. S2: Magnetic susceptibility plots $\chi_M(T)$ and $\chi_M^{-1}(T)$ of (a) $Zn_{0.2}Mn_{0.8}PS_3 \cdot 0.25H_2O$, (b) $Ni_{0.2}Mn_{0.8}PS_3 \cdot 0.25H_2O$ and (c) $Co_{0.2}Mn_{0.8}PS_3 \cdot 0.25H_2O$. The red lines are the least-square fit with Eq (2) as described in text. The blue line is the least square fit with Eq (4) as described in the text.

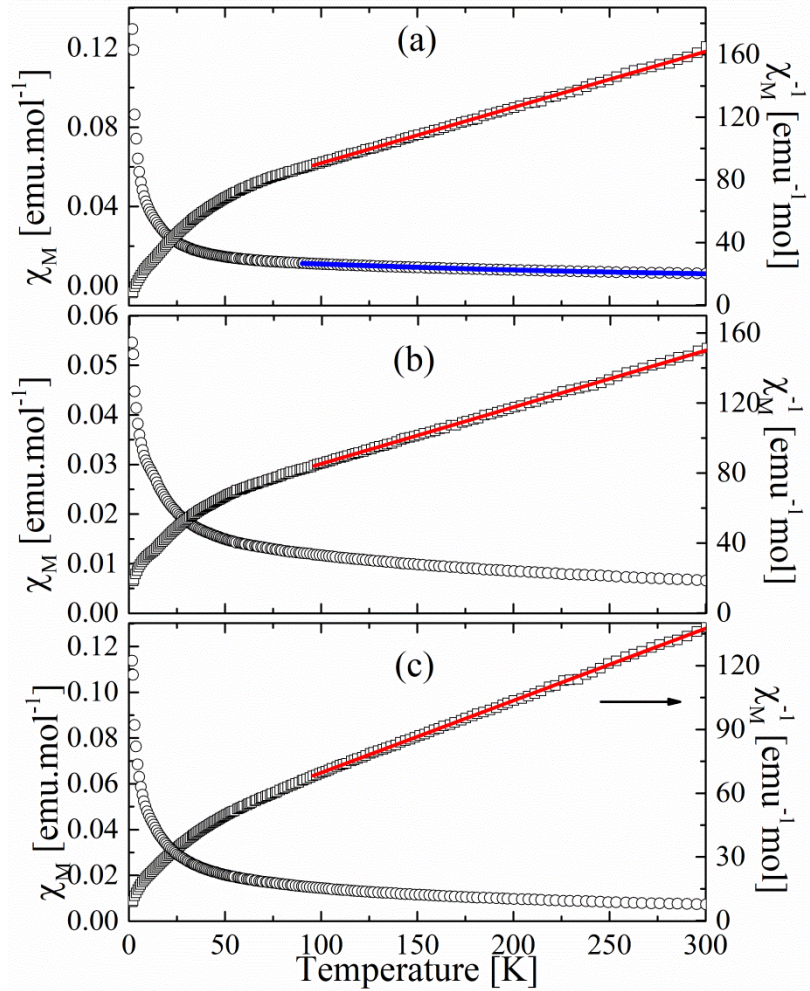


Fig. S3: FC and ZFC susceptibility curves of (a) $Zn_{0.2}Mn_{0.8}PS_3 \cdot 0.25H_2O$, (b) $Cu_{0.2}Mn_{0.8}PS_3 \cdot 0.25H_2O$, (c) $Ni_{0.2}Mn_{0.8}PS_3 \cdot 0.25H_2O$ and (d) $Co_{0.2}Mn_{0.8}PS_3 \cdot 0.25H_2O$.

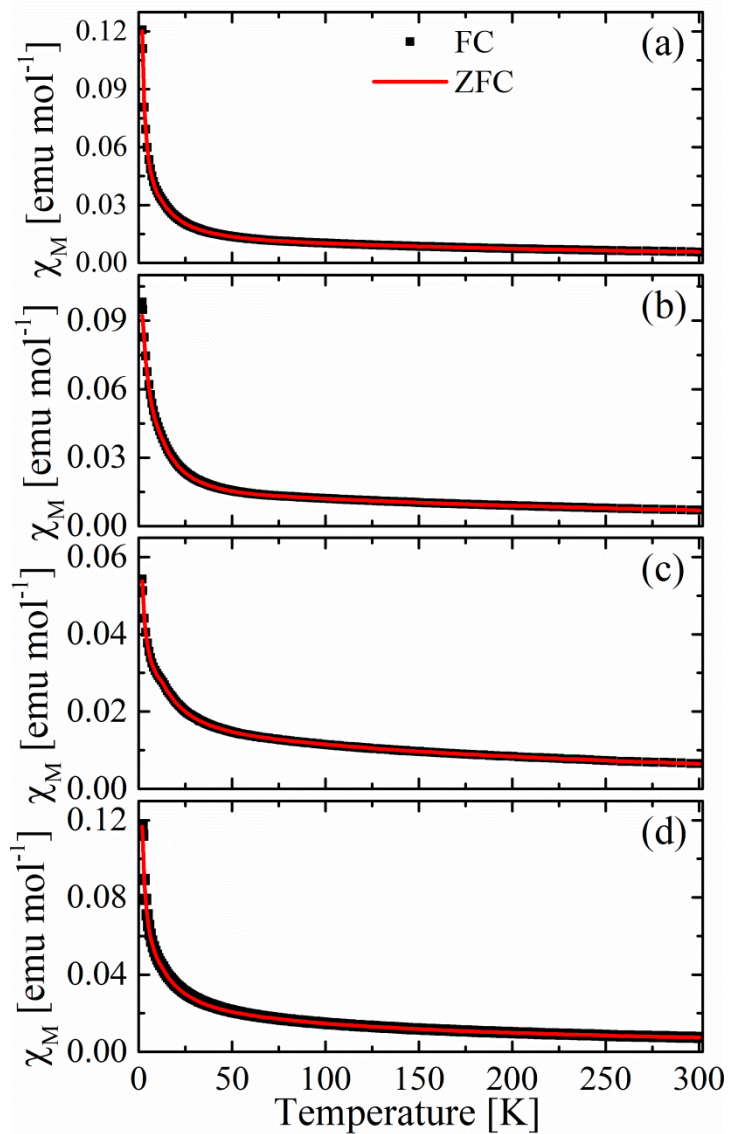


Fig. S4: (a) to (c) Field dependence of magnetization; and (d) to (f) first derivative curves. Measurements made for $\text{Zn}_{0.2}\text{Mn}_{0.8}\text{PS}_3$, $\text{Ni}_{0.2}\text{Mn}_{0.8}\text{PS}_3$ and $\text{Co}_{0.2}\text{Mn}_{0.8}\text{PS}_3$ at different temperatures.

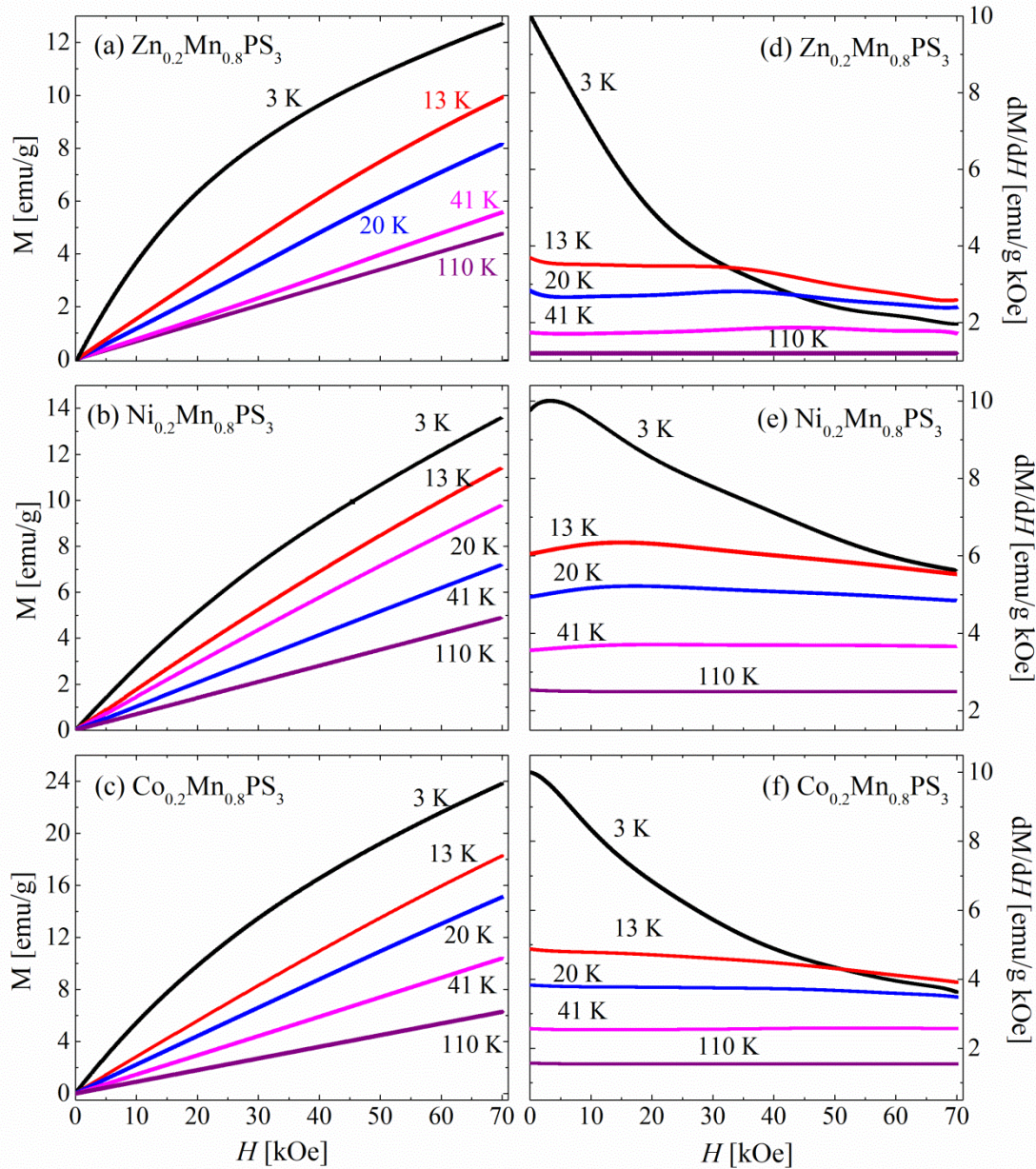


Fig. S5: EPR spectra of (a) $\text{Zn}_{0.2}\text{Mn}_{0.8}\text{PS}_3\cdot0.25\text{H}_2\text{O}$ and (b) $\text{Ni}_{0.2}\text{Mn}_{0.8}\text{PS}_3\cdot0.25\text{H}_2\text{O}$.

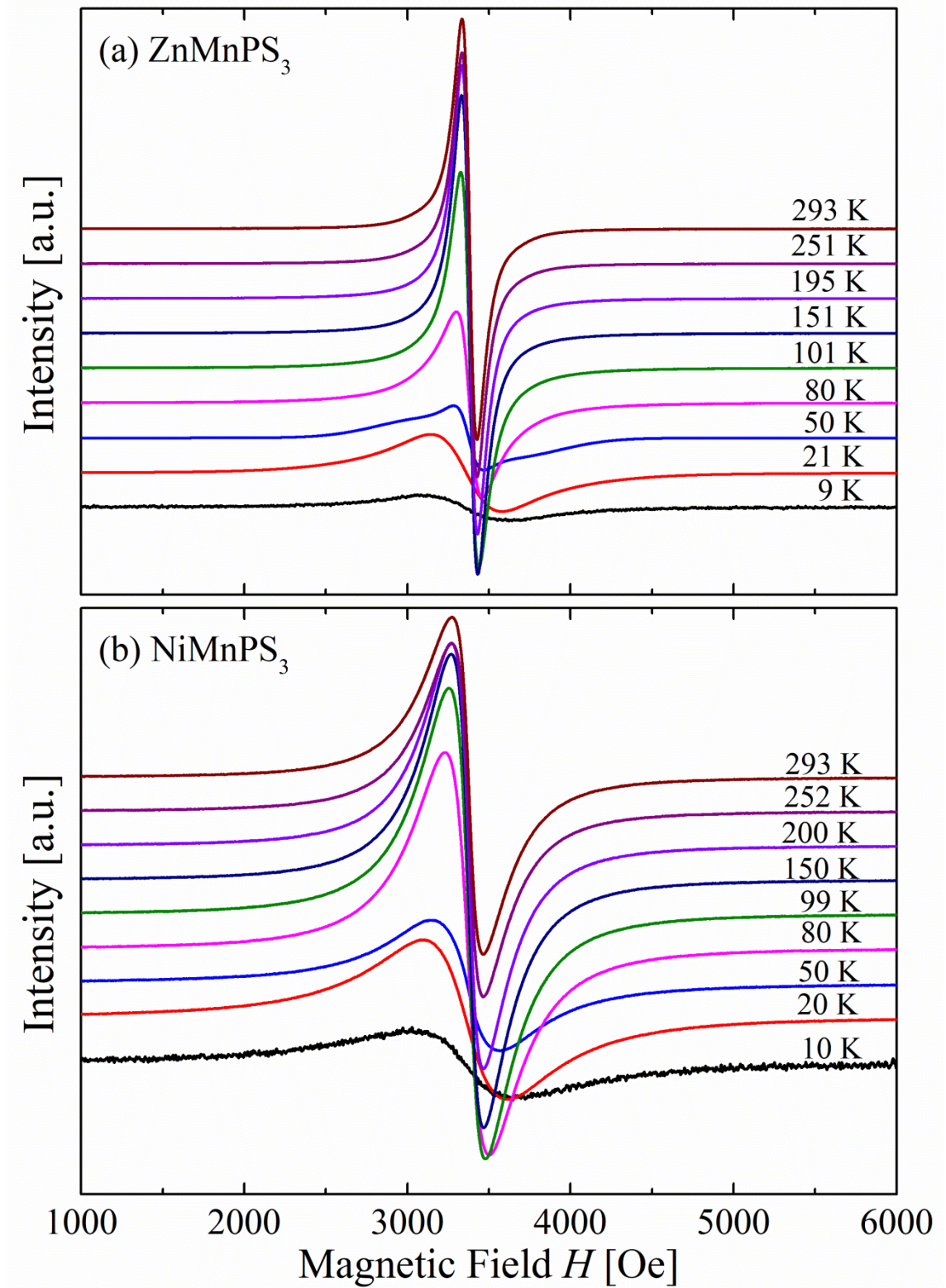


Fig. S6. $I_{\text{DIN}}(T)$ of the studied phases.

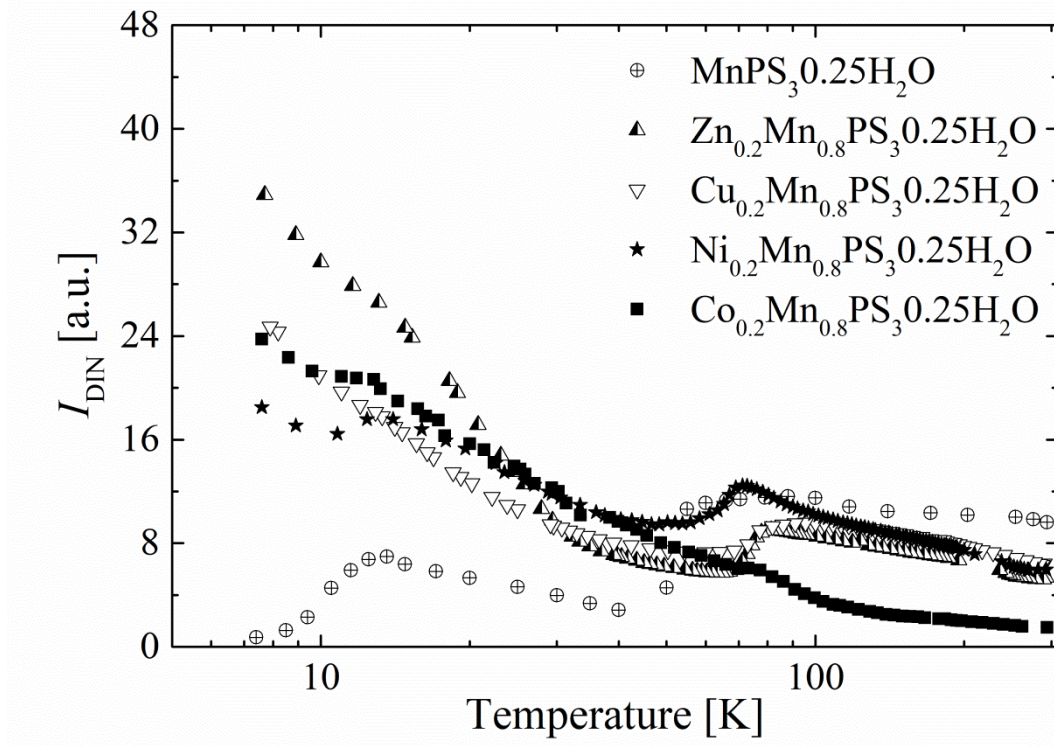
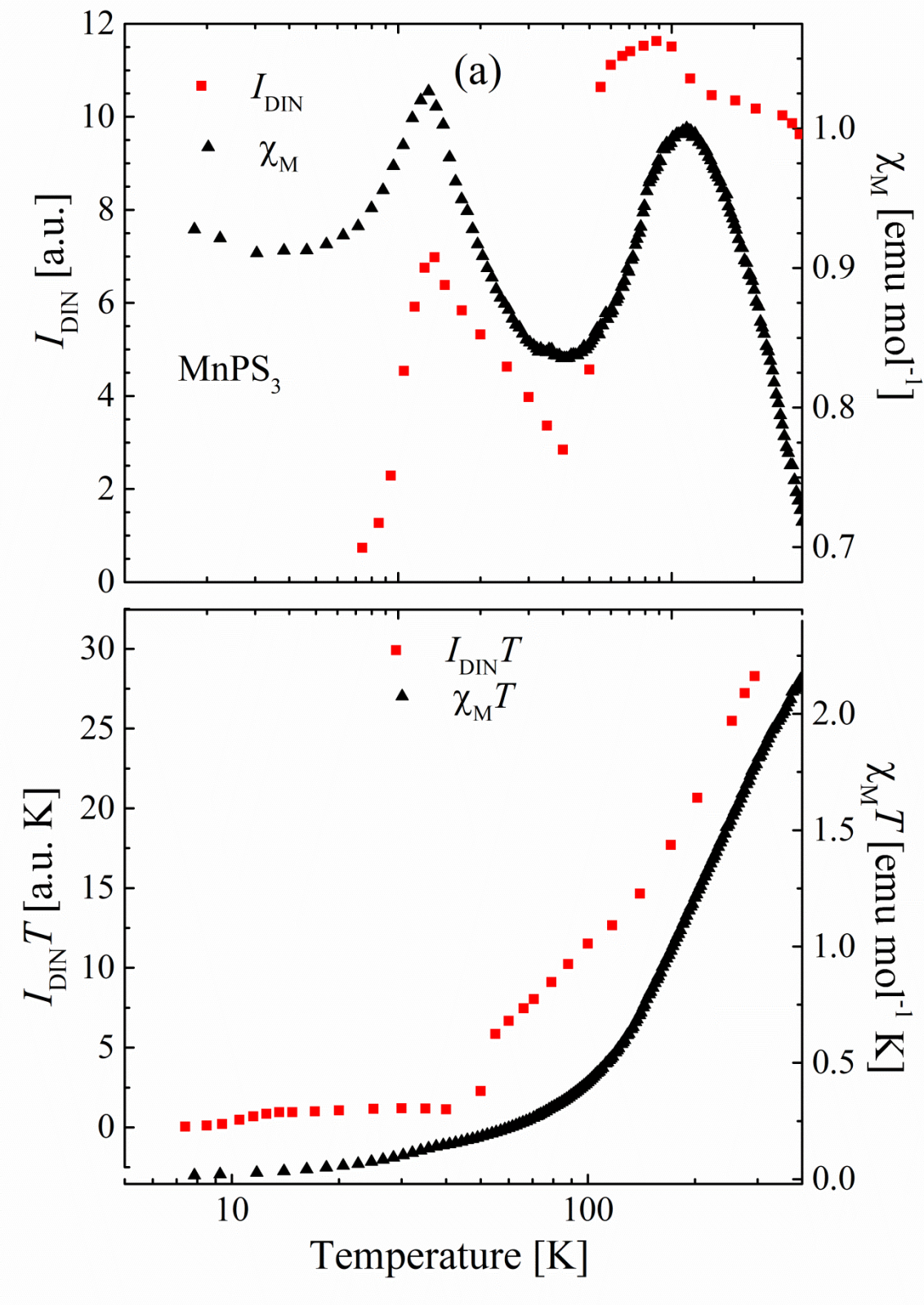
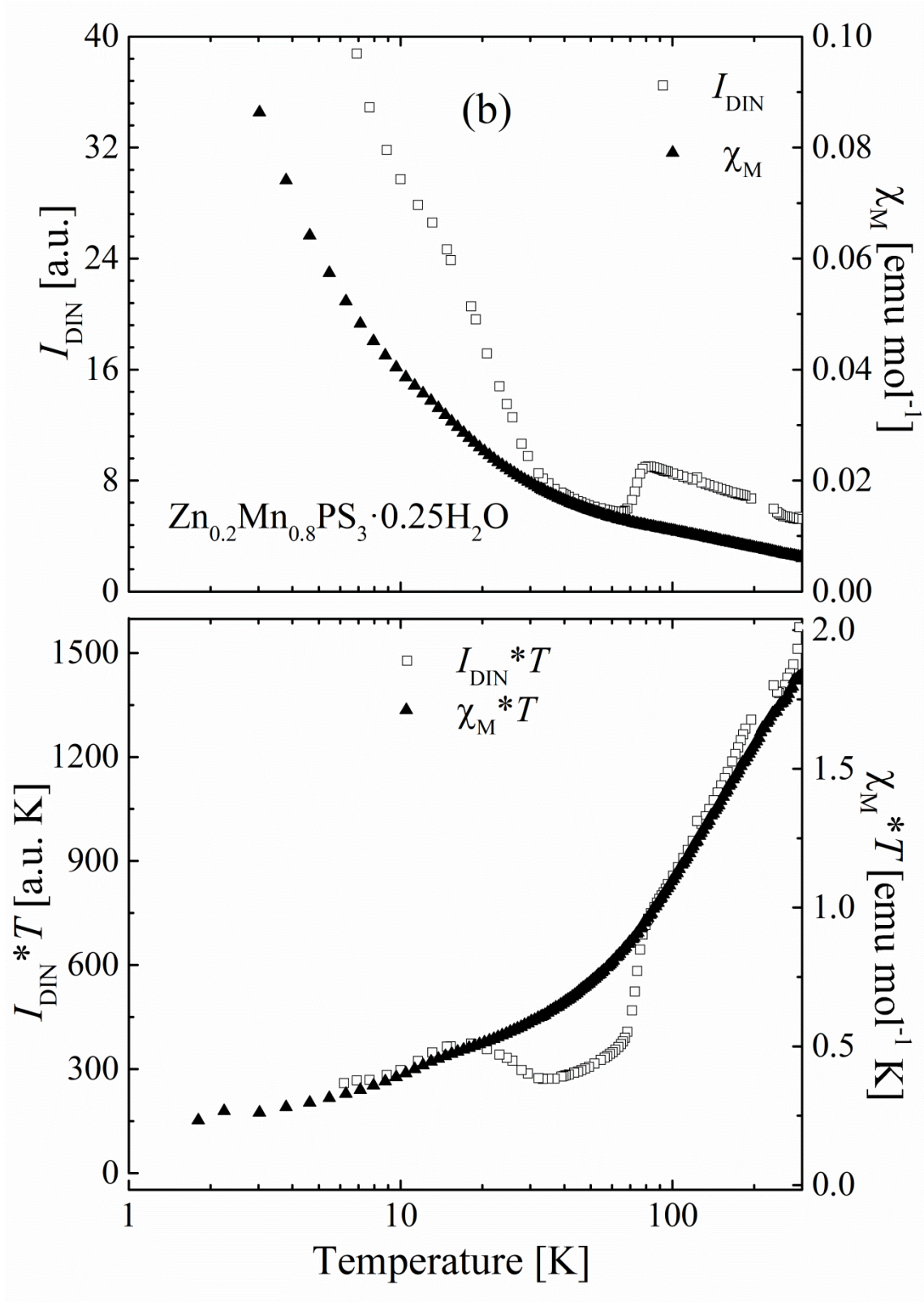
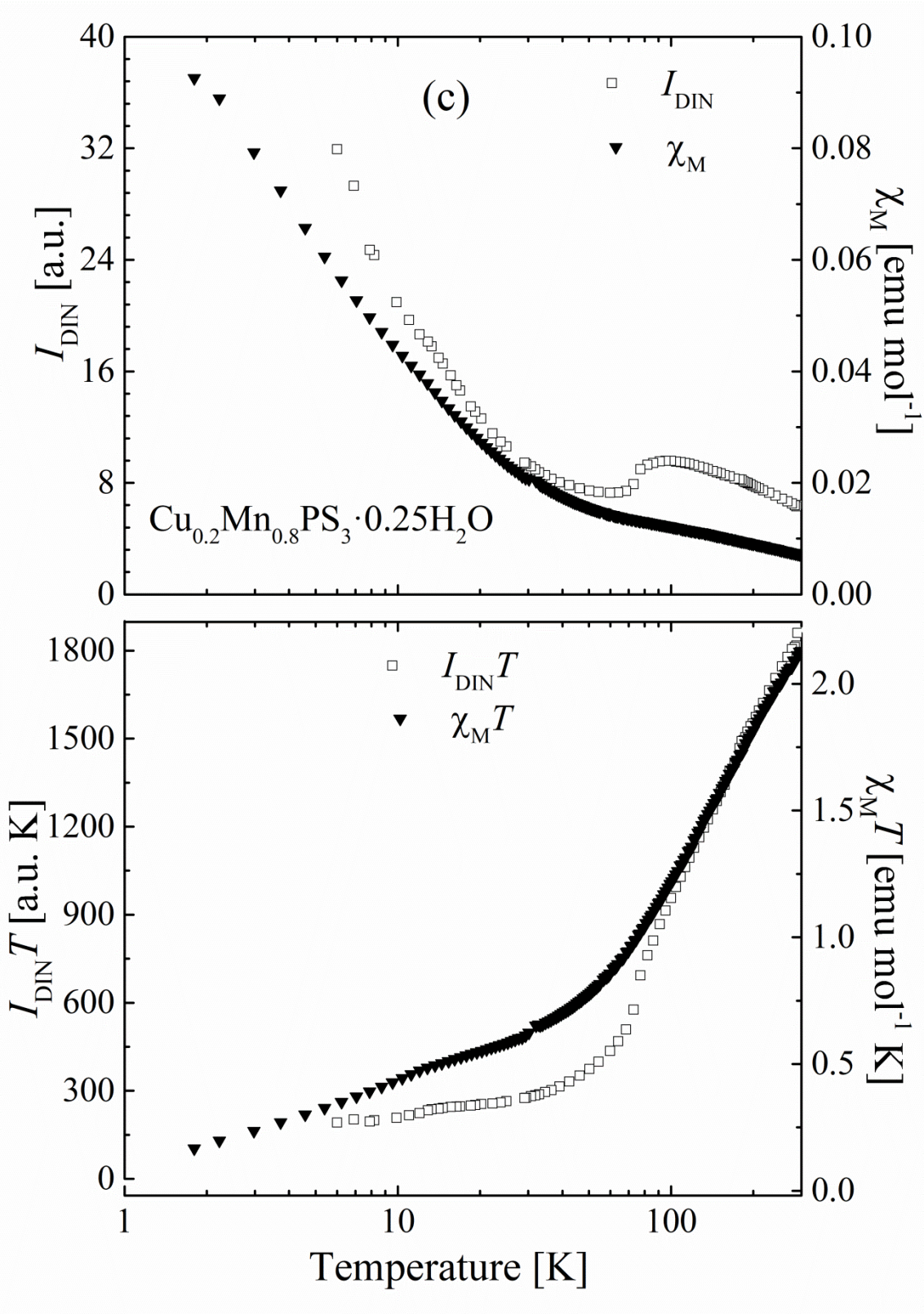
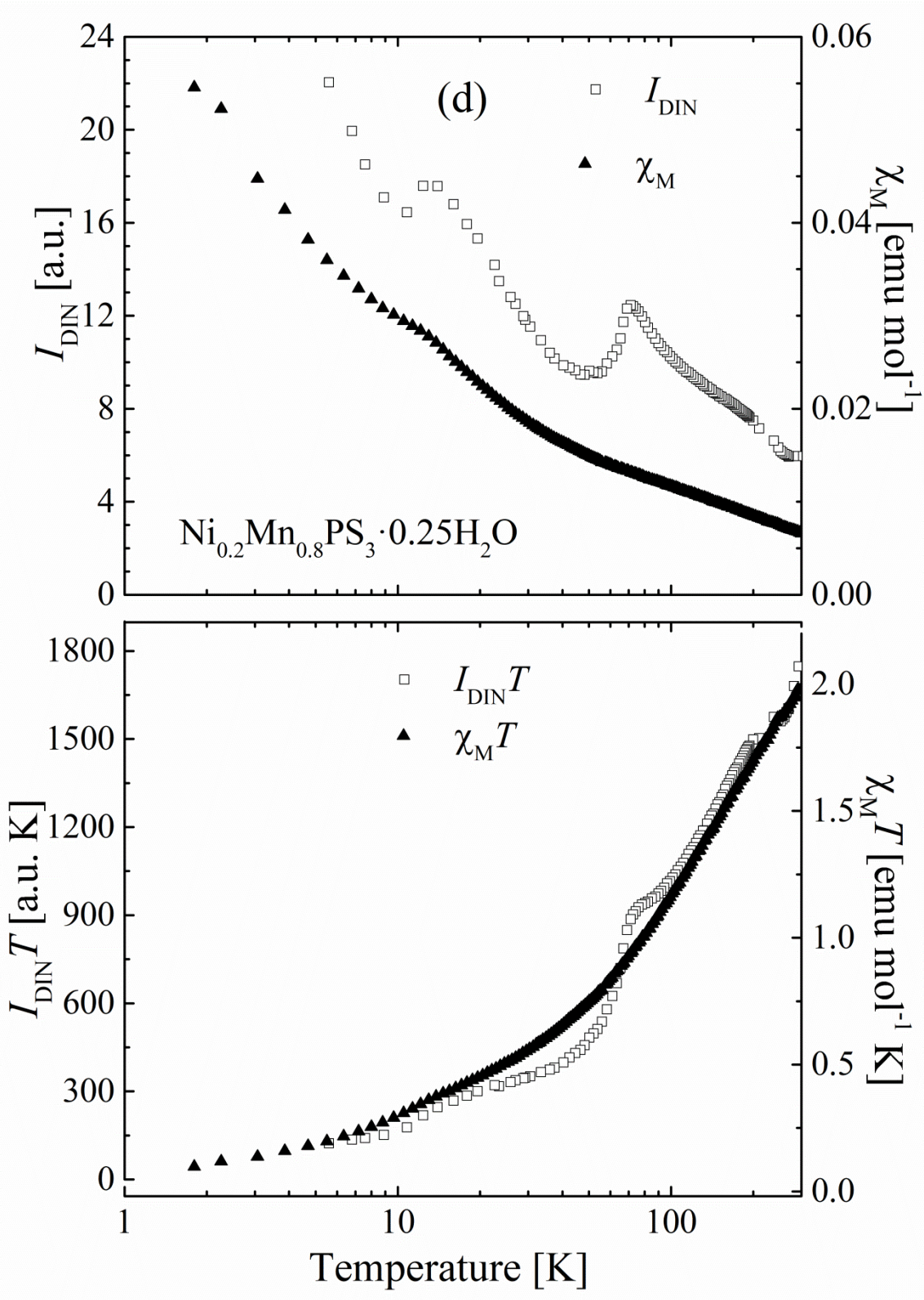


Fig. S7: Comparisons between EPR intensities after double integration (I_{DIN}) with magnetic susceptibility data (χ_M), and EPR intensities ($I_{\text{DIN}}T$) with magnetic susceptibility ($\chi_M T$) temperature product data of pristine and bimetallic phases: (a) MnPS₃, (b) Zn_{0.2}Mn_{0.8}PS₃·0.25H₂O, (c) Cu_{0.2}Mn_{0.8}PS₃·0.25H₂O, (d) Ni_{0.2}Mn_{0.8}PS₃·0.25H₂O and (e) Co_{0.2}Mn_{0.8}PS₃·0.25H₂O.









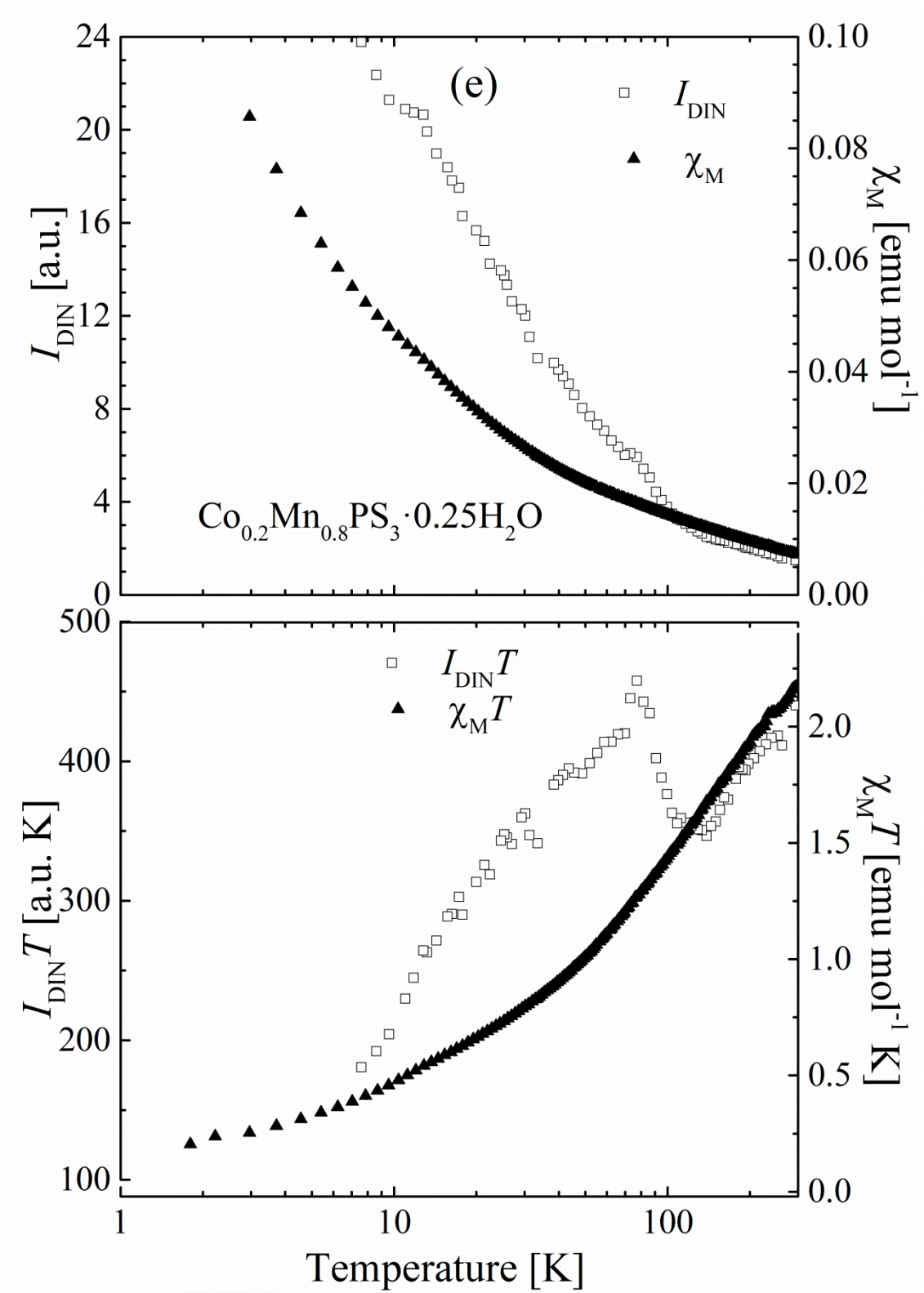
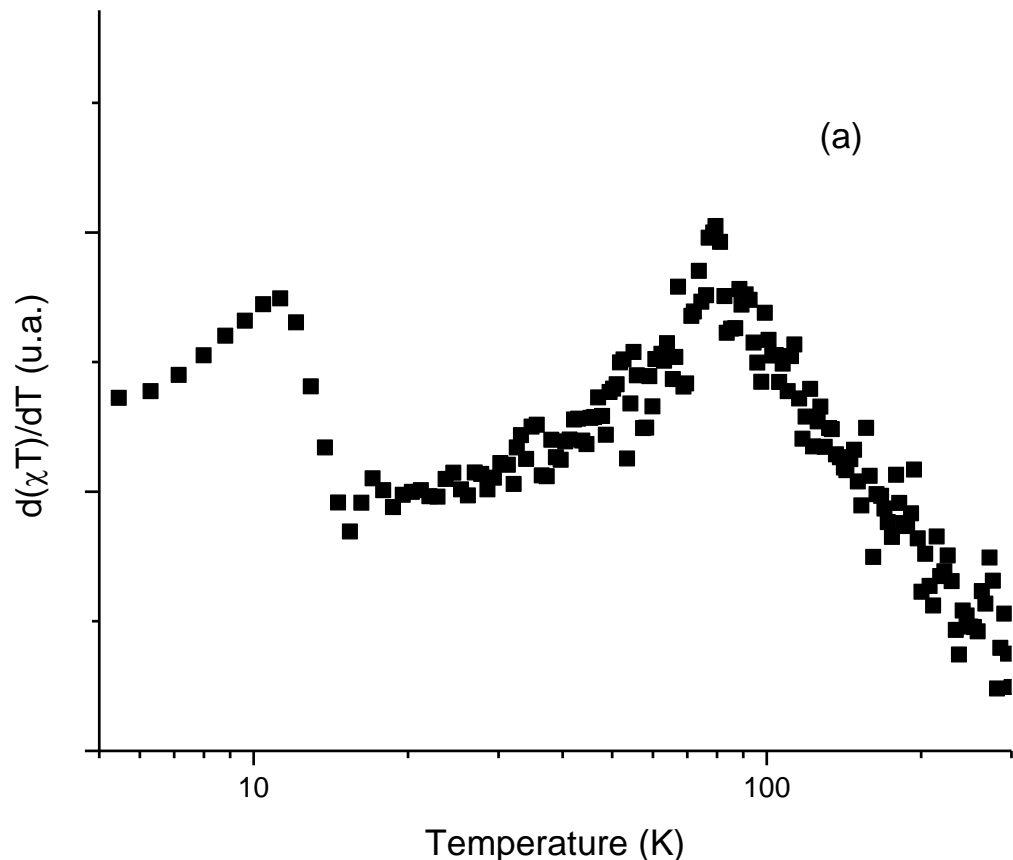
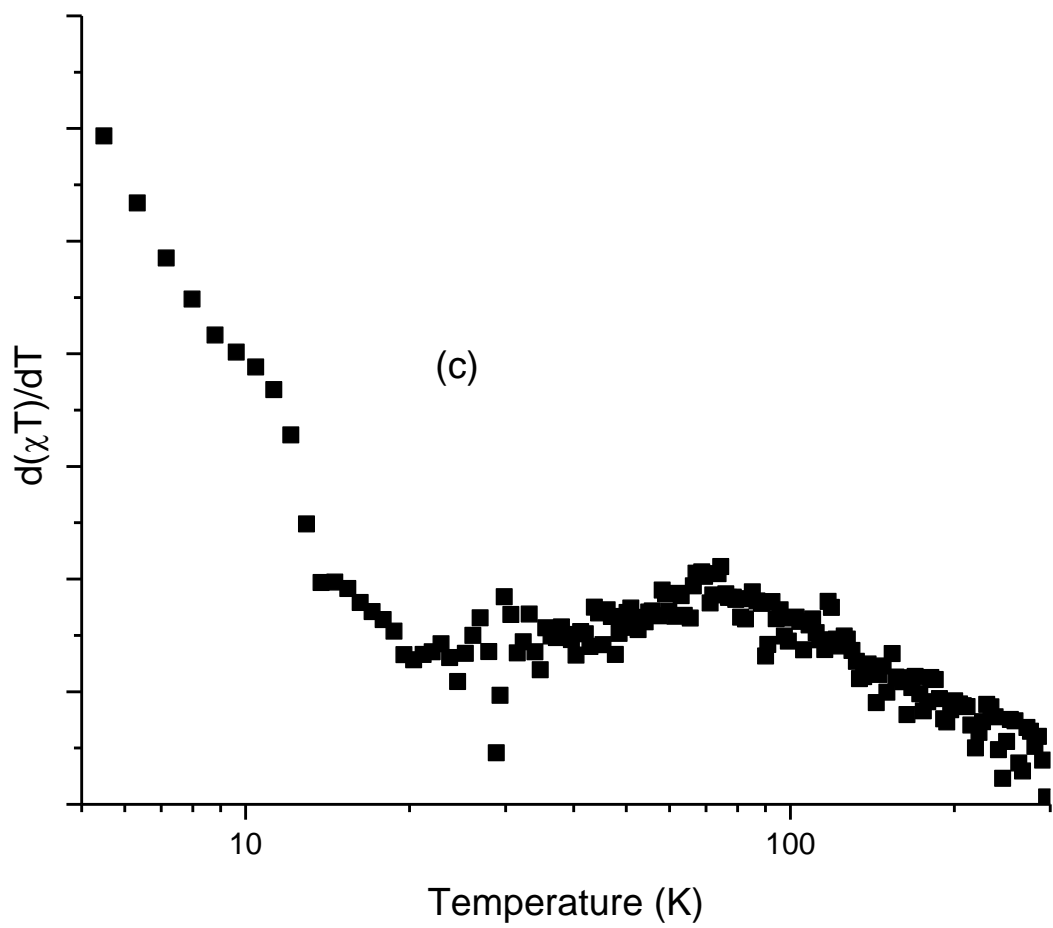
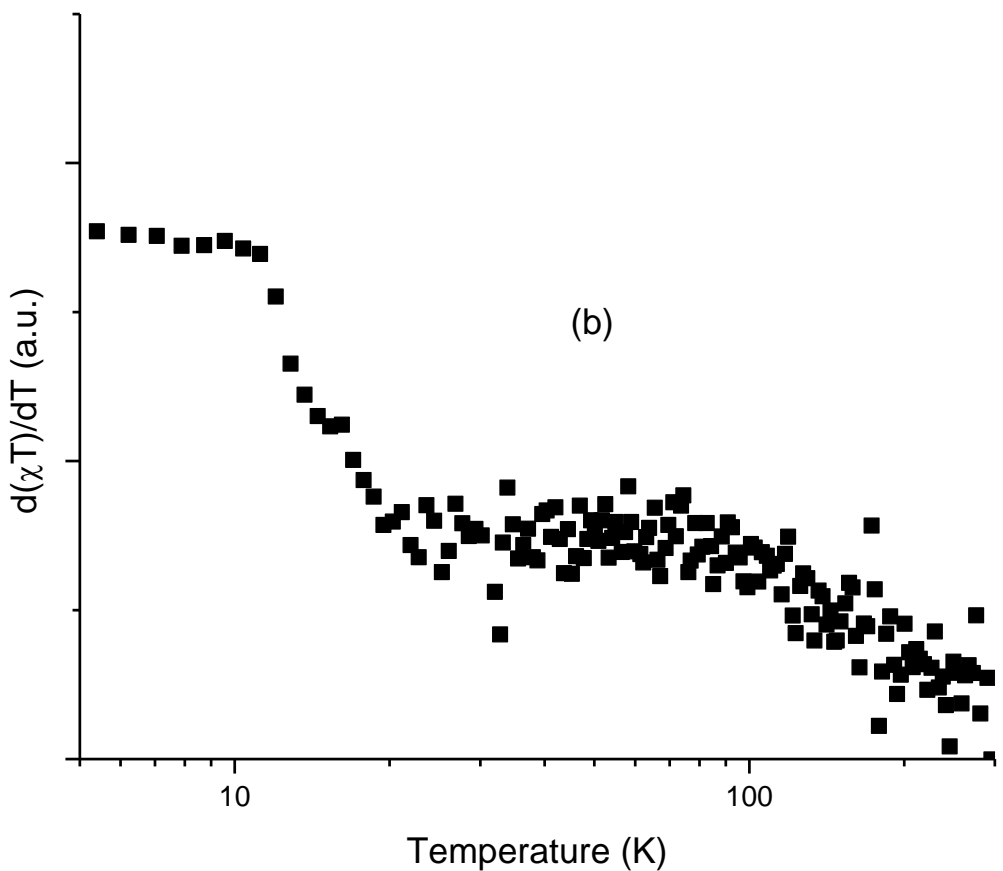
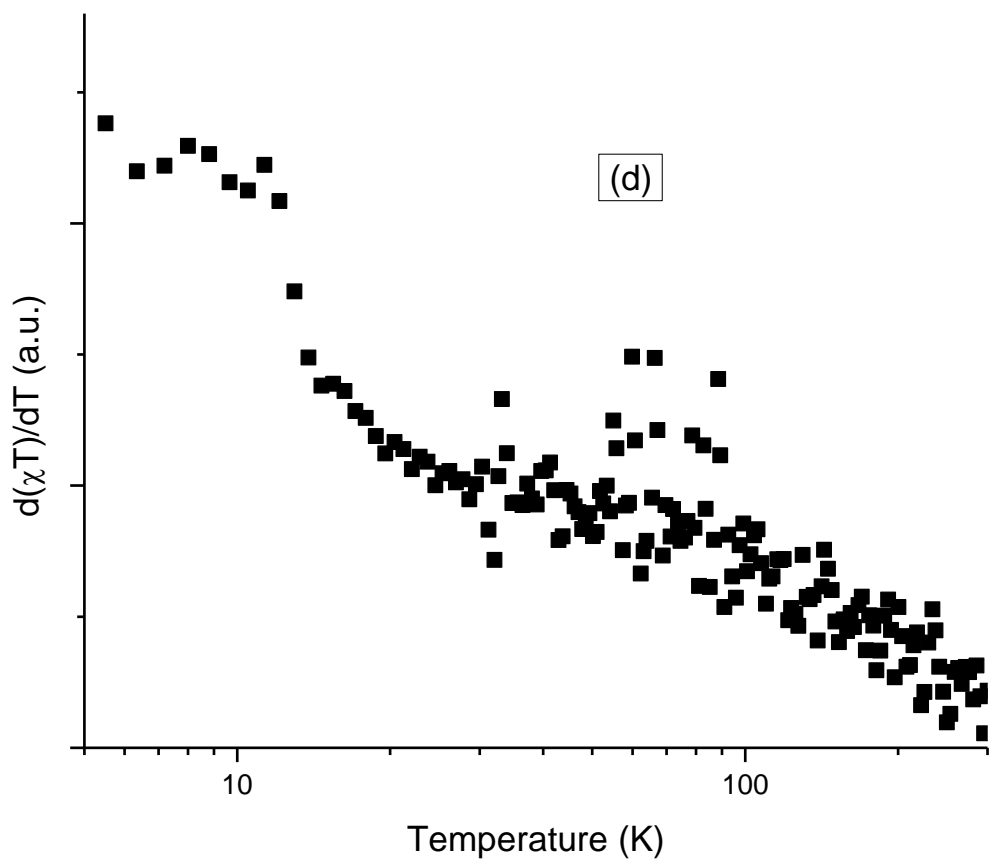
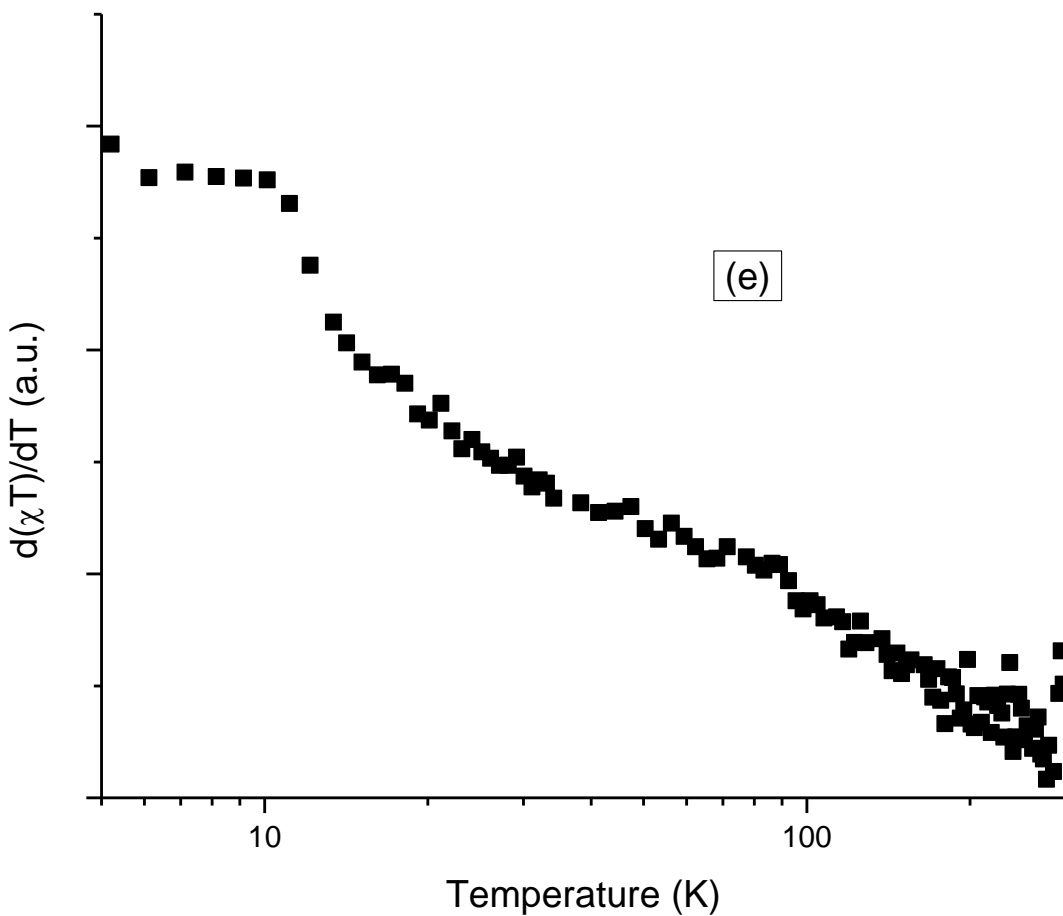


Fig S8. First derivative of the $\chi T(T)$ plot for the pristine and bimetallic phases: (a) MnPS_3 , (b) $\text{Zn}_{0.2}\text{Mn}_{0.8}\text{PS}_3 \cdot 0.25\text{H}_2\text{O}$, (c) $\text{Cu}_{0.2}\text{Mn}_{0.8}\text{PS}_3 \cdot 0.25\text{H}_2\text{O}$, (d) $\text{Ni}_{0.2}\text{Mn}_{0.8}\text{PS}_3 \cdot 0.25\text{H}_2\text{O}$ and (e) $\text{Co}_{0.2}\text{Mn}_{0.8}\text{PS}_3 \cdot 0.25\text{H}_2\text{O}$.









- (1) Evans, J. S. O.; O'Hare, D.; Clement, R. The Structure of Co(.eta.-C₅H₅)₂⁺ and NMe₄⁺ Intercalates of MnPS₃: An X-Ray, Neutron-Diffraction, and Solid-State NMR Study. *J. Am. Chem. Soc.* **1995**, *117* (16), 4595–4606 DOI: 10.1021/ja00121a017.
- (2) Evans, J. S. O.; O'Hare, D.; Clement, R.; Leaustic, A.; Thuéry, P. Origins of the Spontaneous Magnetization in MnPS₃ Intercalates: A Magnetic Susceptibility and Powder Neutron Diffraction Study. *Adv. Mater.* **1995**, *7* (8), 735–739 DOI: 10.1002/adma.19950070812.